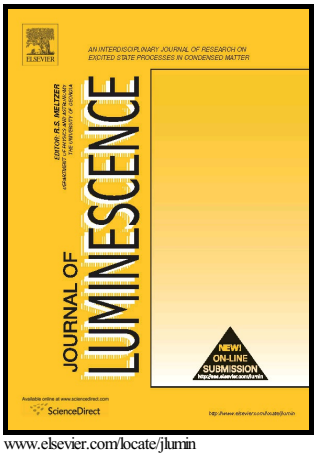

www.elsevier.com/locate/jlumin

$In_xAl_{1-x}N/Al_{0.53}Ga_{0.47}N$ multiple quantum wells on $Al_{0.5}Ga_{0.5}N$ buffer with variable in-plane lattice parameter

Vitaly Z. Zubialevich, Mikalai V. Rzheutski, Haoning Li, Thomas C. Sadler, Shahab N. Alam, Vipul Bhardwaj, Evgenii V. Lutsenko, Gennadii P. Yablonskii, Peter J. Parbrook

PII: S0022-2313(17)30729-9
DOI: http://dx.doi.org/10.1016/j.jlumin.2017.09.053
Reference: LUMIN15061

To appear in: *Journal of Luminescence*

Received date: 30 April 2017
Accepted date: 22 September 2017

Cite this article as: Vitaly Z. Zubialevich, Mikalai V. Rzheutski, Haoning Li, Thomas C. Sadler, Shahab N. Alam, Vipul Bhardwaj, Evgenii V. Lutsenko, Gennadii P. Yablonskii and Peter J. Parbrook, In $_xAl_{1-x}N/Al_{0.53}Ga_{0.47}N$ multiple quantum wells on $Al_{0.5}Ga_{0.5}N$ buffer with variable in-plane lattice parameter, *Journal of Luminescence,* http://dx.doi.org/10.1016/j.jlumin.2017.09.053

$In_xAl_{1-x}N/Al_{0.53}Ga_{0.47}N$ multiple quantum wells on $Al_{0.5}Ga_{0.5}N$ buffer with variable in-plane lattice parameter

Vitaly Z. Zubialevich [1,*], Mikalai V. Rzheutski [2], Haoning Li [1, 3], Thomas C. Sadler [1], Shahab N. Alam [1, 3], Vipul Bhardwaj [1, 3], Evgenii V. Lutsenko [2], Gennadii P. Yablonskii [2], and Peter J. Parbrook [1, 3]

[1] *Tyndall National Institute, University College Cork, Lee Maltings, Dyke Parade, Cork, Ireland;*
[*] *E-mail: vitaly.zubialevich@tyndall.ie*
[2] *B. I. Stepanov Institute of Physics of National Academy of Sciences of Belarus, Nezalezhnasci Ave., 68, 220072 Minsk, Belarus*
[3] *School of Engineering, University College Cork, Cork, Ireland*

Keywords: photoluminescence, InAlN, strain relaxation, type II band lineup

ABSTRACT

The structural and luminescent properties of $In_xAl_{1-x}N/Al_{0.53}Ga_{0.47}N$ multiple quantum wells (MQW) grown on an $Al_{0.5}Ga_{0.5}N$ buffer partially relaxed with respect to an underlying AlN-template are reported. A significant redshift and improvement of ultraviolet (UV) photoluminescence (PL) intensity is found for InAlN MQWs grown on AlGaN buffers with higher relaxation degree. This is attributed to a higher QW indium incorporation as confirmed also by X-ray diffraction (XRD). The nature of room temperature time resolved PL is studied and discussed from the point of view of the possibility of a type I–type II band lineup transition in the InAlN–AlGaN system.

Introduction

Due to the AlGaN bandgap range between 3.4 and 6.0 eV, this alloy is the natural contender for the active region of UV light emitting diodes (LEDs). However, up to now, AlGaN-based LEDs show significantly lower efficiencies in comparison to their InGaN-based counterparts emitting in the visible [1]. Because of the limited availability, small size, and high cost of bulk III-nitride crystals, LED structures are conventionally grown on foreign substrates e.g. sapphire, silicon carbide, and silicon. Due to the lattice mismatch, the resulting material suffers from high dislocation densities (typically mid 10^8 – mid 10^9 cm^{-2}). While, despite the poor crystalline quality, InGaN-based LEDs remain relatively efficient owing to the strong carrier localisation from In composition fluctuations, AlGaN-based LEDs do not have this advantage. This is due to the fact that AlN and

GaN are miscible across the entire range [2] and as a result will only have the inherent composition fluctuations at any random alloy [3] in their ternary compound, which manifests in both a narrower bandwidth of its band-edge emission [1, 3] and a sharper absorption edge [4, 5] in comparison to InGaN [6, 7]. From this point of view the idea of using InAlN (which can be expected to behave more strongly than InGaN) as an active region material for UV LEDs is a potential solution for higher internal quantum efficiencies despite expected difficulties in growth due to the strong differences in optimal growth conditions of the individual binaries [8].

Recently, we reported efficient room temperature UV photoluminescence from InAlN/AlGaN MQWs grown by quasi-two temperature metalorganic vapour phase epitaxy (MOVPE) where InAlN wells and AlGaN barriers are deposited at significantly different temperatures [9]. To protect QWs from losing indium during the temperature ramp to the barrier temperature, thin AlGaN cap layers of optimised thickness have to be deposited straightaway after each well. More recently, photoluminescence (PL) properties of such $In_xAl_{1-x}N/Al_{0.59}Ga_{0.41}N$ MQWs with different In content in them were investigated, and it was found that the highest PL efficiency corresponds to QWs emitting at ~340 nm (18% of In), while a further increase of indium content leads to a sharp deterioration of the luminescence from QWs due to their mechanical relaxation with respect to AlGaN buffer/barriers [10]. In addition to the widely used variation of the growth temperature as applied in [10], other methods of In-content control in III-nitrides are known, such as change of In/III [11, 12] and V/III ratios [13], varying the growth pressure [11, 14] and the growth rate [12]. Here we report a possibility to achieve this in InAlN/AlGaN MQWs by alteration of in-plane lattice parameter *a* of $Al_{0.5}Ga_{0.5}N$ buffer on which the QW stack is grown. As a part of this study we report mechanical strain condition of thick $Al_{0.5}Ga_{0.5}N$ layers grown on AlN/sapphire templates after the strain-relieving GaN interlayers of different nominal thickness. The effect of AlGaN buffer relaxation (and thus its in-plane lattice parameter) on luminescent properties and mechanical relaxation of InAlN QWs (especially those with In content of above 18%) is investigated by means of time integrated/resolved PL and XRD.

Experimental

InAlN/AlGaN MQW heterostructures studied here were grown in a 3x2" AIXTRON MOVPE reactor using trimethylgallium, trimethylaluminium, trimethylindium and ammonia as precursors. Hydrogen was used as a carrier gas for all the structure with the exception of the MQW stack which was grown in a nitrogen ambient. Initially, 2.5 μm thick AlN layers were deposited on *c*-plane sapphire substrates as described in [15], followed by a thin GaN (d_{GaN} = 0-20 nm) interlayer (IL) similar to that reported by Wang et al. [16]. After that, an approximately 1 μm thick AlGaN layer was grown, followed by an MQW stack consisting of five 2 nm thick $In_xAl_{1-x}N$ wells and 8 nm thick $Al_{0.53}Ga_{0.47}N$ barriers. Growth conditions for the MQW stacks were fixed for all samples: in particular, QWs and barriers were grown at 755°C and 1110°C respectively. To allow the high temperature barrier growth, deposition of a thin AlGaN cap layer immediately after the preceding well (at the QW-temperature) was applied to prevent In desorption from the well, as described in [9]. A high V/III ratio (3740) and a TMIn/TMAl ratio of 0.5 were used to grow the InAlN QWs.

AlGaN strain analysis was carried out based on in-situ wafer curvature using a LayTec EpiTT/EpiCurve system and ex-situ X-ray diffraction (XRD) using a PANalytical X'pert PRO XRD kit. Particularly symmetric 0002 ω-2Θ scans and asymmetric 10-15 reciprocal space maps were carried out to determine the indium content in QWs and in-plane lattice parameters of AlGaN buffers.

For the time integrated PL measurements, samples were excited with the second harmonic of 488 nm line of a cw Ar-ion laser and the emission detected using a Horiba iHR320 imaging spectrometer equipped with a CCD camera. A diode-pumped Yb:KYW femtosecond laser was used to excite the studied samples in the case of time resolved PL. For this purpose the fourth harmonic of its emission was used (λ = 258 nm, f = 62 kHz, τ = 140 fs, E_p = 0.28 μJ) and the PL was detected with a C4334 Hamamatsu streak camera equipped imaging spectrometer.

The surface morphology of the GaN IL was analysed using a Veeco MultiMode V atomic force microscope in tapping mode.

Results and discussion

$Al_{0.50}Ga_{0.50}N$ buffer layers with different degrees of relaxation with respect to their AlN/sapphire templates were achieved by growth of varied thickness GaN interlayers (IL) in between. No significant effect on the in-situ curvature was observed for GaN IL thicknesses d_{GaN} up to nominally 7.5 nm in comparison to the sample without it (not shown). However, thicker ILs led to an obvious change indicating a clear reduction of the compressive strain ultimately converting it into a tensile strain (Fig. 1) leading to heavy cracking for the thickest GaN IL of nominally 20 nm. This is due to rapid in-plane relaxation of the GaN IL because of the large mismatch in *a* lattice parameters between GaN and AlN [17].

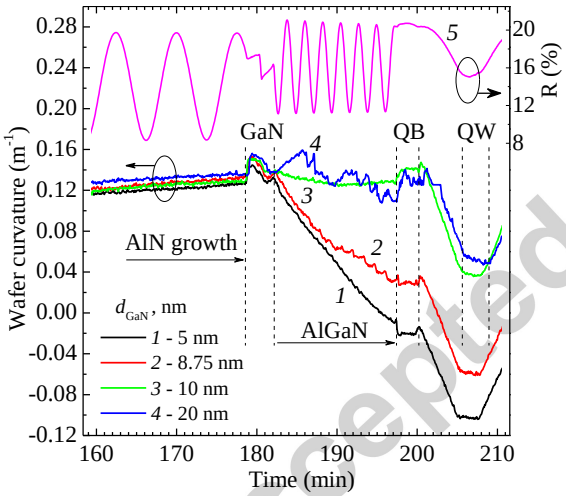

Fig. 1. – In-situ curvature data for samples grown with different GaN IL thicknesses (1-4). Curve 5 represents in-situ reflectance (using a 650 nm LED) for one of them.

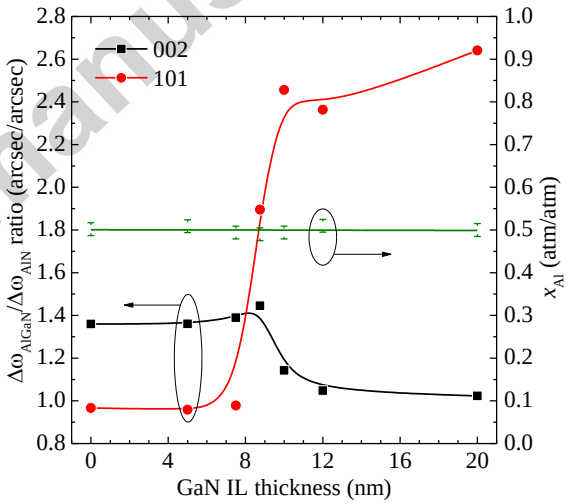

FIG. 2. – Ratios between FWHMs of XRD reflectance of AlGaN buffer and underlying AlN template (filled symbols) and Al-content in the AlGaN (hollow diamonds) as a function of d_{GaN}.

While the introduction of the GaN IL did not lead to any noticeable change in the AlGaN composition (open diamonds in Fig. 2), it significantly increased the 10-11 XRD full width half

maximum (FWHM) for the AlGaN buffer in comparison to that of underlying AlN (circles in Fig. 2). The latter observation together with a slight decrease in FWHM of the 0002 diffraction peak (squares in Fig. 2) indicate the formation of almost pure edge type dislocations in the GaN ILs as the main mechanism of the observed strain relaxation.

It is interesting to note that the observed here effect of thin GaN IL on AlGaN crystalline quality differs significantly from that reported in Ref. 16, where dislocations threading from AlN template were seen to form loops within the GaN IL and to be partially filtered by it. This positive effect may not happen in the present case owing to a number of possible factors: A significantly higher AlN quality (typical dislocation densities are $1.5\text{-}2.5\cdot10^{8}$ cm^{-2} and $1.5\text{-}2.5\cdot10^{9}$ cm^{-2} for screw and edge types, respectively) makes the dislocation looping difficult through the larger average distance between them; an initial 3D growth of GaN (see below) may also prevent the looping. Additionally, AlGaN in our case is of essentially higher Al content (50% vs. 25% for which dislocation filtering was observed in [16]) and thus has higher lattice mismatch with GaN, so that even filtering of TD by GaN does not prevent formation of new misfit dislocations within the AlGaN.

It is noteworthy that for direct (or with only a thin GaN IL) growth of AlGaN on AlN despite of strong built-in tensile strain, no additional edge dislocations are generated, but instead the material shows an increased 0002 FWHM suggesting formation of extra screw dislocations. In contrast, in the case of AlGaN intentionally relaxed by mean of GaN IL, the driving force for the screw dislocation formation diminishes, and their density in it decreases down to the level found in the AlN template.

While a theoretical estimation for critical thickness of GaN layers grown on AlN substrate gives only few nanometers [18], the fact that initial relaxation takes place in the present case not earlier than at $d_{GaN} = 7.5$ nm can be explained by considering GaN IL surface morphology. A separate sample with nominally 10 nm thick GaN on top of an AlN/sapphire template was prepared by cooling it down in a nitrogen/ammonia ambient. It was investigated by AFM, as shown in Fig. 3,

and rather than a smooth surface, a developed one in the form of hillocks with the average height of 20 nm was observed. Besides the delayed plastic relaxation, such a hillocky surface is most probably responsible also for not observing a distinct GaN-related peak in 0002 ω-2Θ XRD scans for the samples with d_{GaN} < 12 nm (not shown).

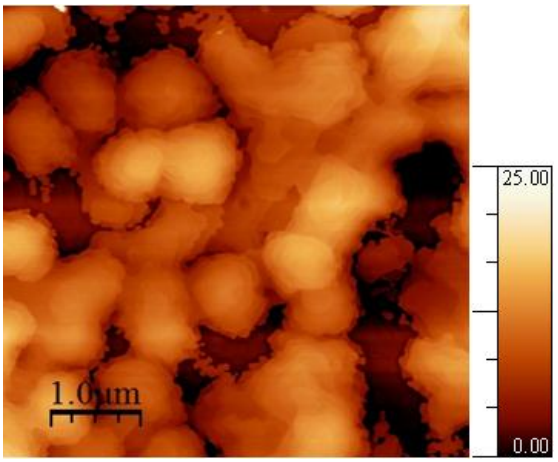

Fig. 3. – AFM image of nominally 10 nm thick GaN layer grown on AlN-template.

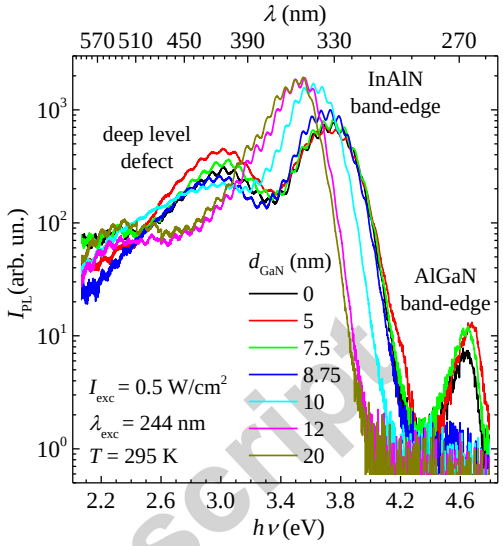

Fig. 4: RT PL spectra of InAlN/AlGaN MQW structures with different thicknesses of GaN IL.

The PL of InAlN/$Al_{0.53}Ga_{0.47}N$ MQWs are shown in Fig. 4. Generally, the room temperature (RT) time integrated PL spectra consist of a mid-UV AlGaN band at 4.65 eV, a near UV QW-related band in the 3.5-3.75 eV range and two wide deep-level-defect (DLD) bands located in the visible (Fig. 4). The exact mechanism of the DLD-related band is not fully clear but, as discussed in our previous work, the bands originate mostly from the AlGaN buffer/barriers [9].

A systematic variation in PL peak position and intensity of the QW-related peak is clearly observed. As d_{GaN} increases beyond around 8 nm the peak redshifts by about 250 meV and enhances in intensity by around a factor of 2.4 (Fig. 5). At the same time, the 3 eV DLD band and the AlGaN band-edge peak diminish for thicker GaN ILs. The same dependence of QW-related emission efficiency on its spectral position was observed in our recent study [10] on similar structures with $In_xAl_{1-x}N$ QWs grown at varied temperatures to vary indium content in them.

As the AlGaN buffer (of roughly the same composition) is relaxed differently with respect to the underlying AlN-template as a function of d_{GaN}, this provides different strain conditions for InAlN grown on it due to a different in-plane lattice mismatch. This apparently leads to an alteration in the indium incorporation rate in our QW samples. We believe the observed phenomenon is related to the strain induced compositional pulling effect [19,20,21,22-23], where it is assumed a mechanism perturbing the alloy composition towards minimisation of the lattice mismatch between the epitaxial layer and its substrate. To examine this we analysed XRD data on 002 ω-2θ reflectance to extract estimated indium contents x_{In} in QWs of the samples and additionally measured 105 reciprocal space maps to determine the in-plane AlGaN lattice parameter, a_{AlGaN}. Further, to eliminate the run-to-run variation of the pyrometer determined QW growth temperature ΔT_{QW} (which was ±3°C for all samples, except for d_{GaN} = 20 nm where it was –10°C), an appropriate correction ($\Delta x_{In} = \Delta T_{QW} \cdot dx_{In}/dT$, where the derivative $dx_{In}/dT = 0.0943$ was taken from [10]) was applied to the XRD determined QW indium contents x_{In}. To estimate the relaxed InAlN in-plane lattice parameter and the actual mechanical strain ($\varepsilon_{xx} = \varepsilon_{yy} = (a_{AlGaN} - a_{InAlN})/a_{InAlN}$) of our QWs, the as measured (not corrected) indium content and a linear interpolation (Vegard's law) between AlN (0.3113 nm [4]) and InN (0.35377 nm [24]) endpoints were used. The obtained results presented in Fig. 6 show that the QW indium content does indeed depend on its mechanical strain state. Particularly, it decreases with increased compressive strain i.e. the strain modifies QW composition towards reduction of itself as in the case of the strain induced compositional pulling effect. This finding is qualitatively in line with previously reported results for In-containing III-nitrides [21, 22].

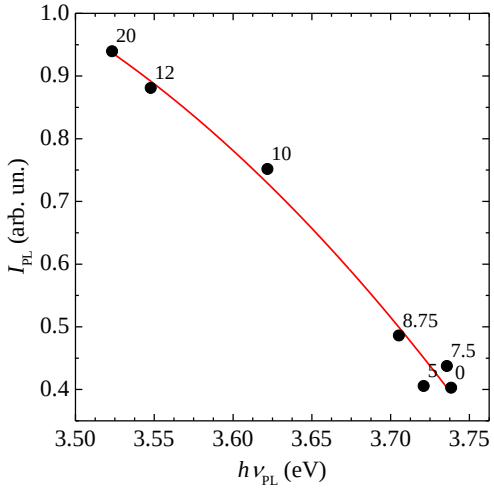

Fig. 5. – Dependence of PL intensity of QW-related PL band on its spectral position for samples grown with different thickness of GaN IL (are given in nanometers next to the datapoints).

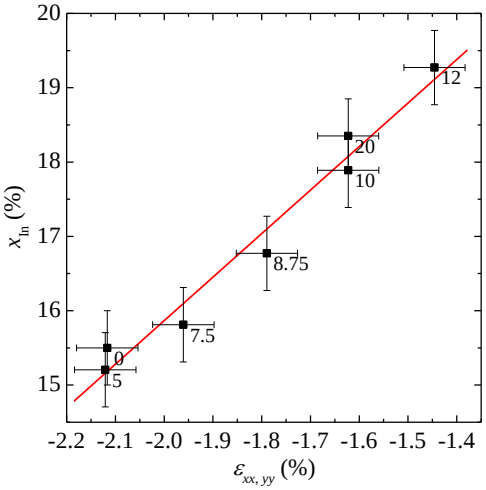

Fig. 6. – Growth temperature corrected QW indium content as a function of InAlN strain. (Data point values are GaN IL thicknesses in nm)

It is worth considering in more detail the data presented in Fig. 5. One can see that PL intensity increases as the peak position redshifts with higher indium incorporation. Two features are of note: First, the increase of PL efficiency with the redshift is similar to that observed in [10] and takes place despite the strong increase in total dislocation density (see discussion of Fig. 2 above); second, there is an absence of the sharp reduction in PL efficiency at In content exceeding 18%, in contrast to the previously observed behaviour of the same type QWs [10]. The first feature clearly indicates a weak sensitivity of the PL efficiency to dislocations threading from the substrate/buffer, which can serve as another confirmation of the strongly localised nature of non-equilibrium carriers participating in radiative recombination in InAlN. It is in contrast to AlGaN whose weak PL band observed in the case of thin GaN ILs diminishes completely as dislocation density increases (comp. data in Fig. 2 and Fig. 4). The second observation can be explained by the absence of plastic deformation within QWs due to the reduced InAlN strain owing to the increased in-plane lattice parameter of the AlGaN buffer (and thus barriers) in comparison to the case described in [10].

To investigate further, time resolved PL measurements of the samples were carried out and analysed. Samples show non-monoexponential PL decays (Fig. 7) with instantaneous lifetimes ranging from 0.8-2 ns immediately after the excitation pulse (depending on excitation level) up to 55-120 ns later on (ultimate lifetime).

Under pulsed excitation, general trends across the series are that the samples with thicker GaN ILs: (I) demonstrate brighter and longer wavelength PL (similar to the cw excitation case, comparable with Fig. 4, Fig. 5); (II) are characterised by faster ultimate PL lifetimes (measured > 120 ns after laser pulse); (III) show ultimate PL lifetimes that are almost independent of excitation level. Additionally, with increased excitation, for all samples: (IV) the average contribution of fast PL decay increases, reducing the average PL lifetime; and (V) the total (time integrated) PL intensity increases sublinearly.

In [10] we proposed transition from type I to type II lineup in InAlN/AlGaN QWs (holes are no longer confined in the InAlN while electrons still are) with decreasing In content as a possible mechanism of the PL efficiency degradation, and some evidence was provided to support this conjecture. The above described observations may serve as a further support of this view.

Initially after excitation pulse, photogenerated carriers thermalise and occupy localised states in InAlN. Immediately after the thermalisation, all In-rich regions contribute to the PL equally (in proportion to the number of carriers ended up there). As the sites of QWs where carriers are localised are not equal, the relative their contribution to the PL changes with time. Particularly, those regions with higher probabilities of nonradiative recombination in them and/or higher carrier escape rate will contribute less and less with time leading to the observed non-monoexponential decay. We attribute thus the longer lifetime observed at a later stage of PL transient to the intrinsic carrier lifetime due to their spontaneous radiative recombination in those localised states where the nonradiative processes are insignificant. At the same time, apparently the initial fast recombination is determined just by their contribution.

It is worth noting that for $In_xAl_{1-x}N/Al_{0.53}Ga_{0.47}N$ QWs with $x \approx 0.14$ polarisation matching occurs (the built-in electric field due to spontaneous polarisation and the corresponding strain induced piezoelectric component cancel each other). Thus one would expect a shorter radiative lifetime for samples with indium content closer to 14% because of reduced quantum confinement Stark effect (QCSE). In contrast to this expectation, in our case the ultimate radiative lifetime (measured at $t > 120$ ns) increases with decrement of x_{In} towards this polarisation matching value (Fig. 8). However electron and hole wave functions overlapping (and thus the recombination probability and the corresponding radiative lifetime) is determined not only by QCSE. An increasingly strong spreading of holes' wave functions to the AlGaN barriers in virtue of vicinity to the transition from type I to type II band lineup in QWs with lower indium content would have a similar effect on the overlap even without band bending. At the same time this should generally improve the nonradiative recombination due to a higher probability of holes to meet defects in AlGaN in full agreement with our observation (Fig. 8).

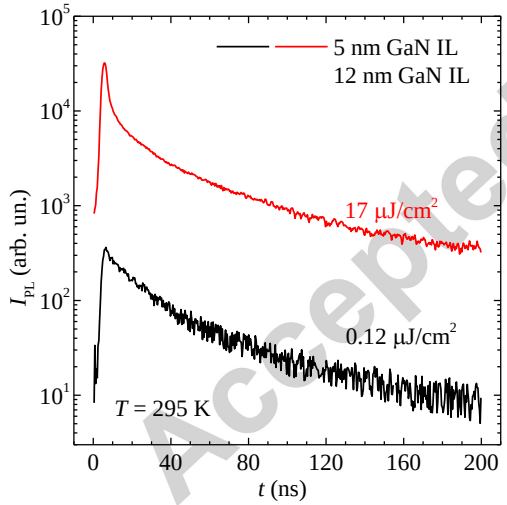

Fig. 7. – RT PL transients for two InAlN/AlGaN QW samples at two different excitation levels.

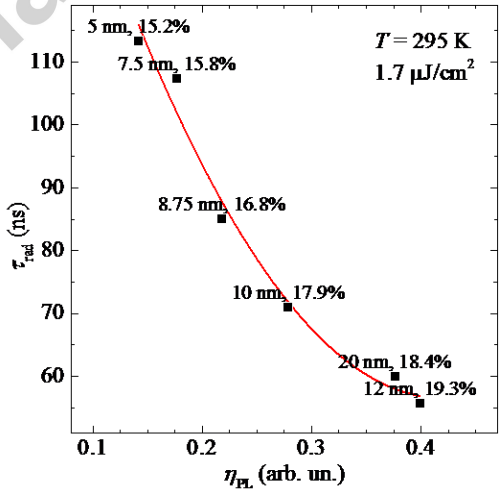

Fig. 8. – Radiative lifetimes of carriers in samples grown with different GaN IL plotted with respect corresponding PL efficiencies. IL nominal thicknesses and QW indium contents are given next to the

datapoints.

With increased excitation level, an enhancement of relative contribution of the fast time components in the overall PL transient occurs, as seen qualitatively from Fig. 7 and quantitatively from the upper part of Fig. 9. The average lifetime in Fig. 9 is defined as the ratio $\langle\tau\rangle = I_{\mathrm{int}}/I_0$, where I_0 is the maximal PL intensity (intensity at the very beginning of PL decay) and the integral intensity I_{int} is given by the following integral:

$$I_{\mathrm{int}} = \int_{t_0}^{t_{max}} I(t)dt,$$

where t_0 = 6 ns is the time corresponding to the maximal PL intensity ($I_0 = I(t_0)$) and t_{max} = 200 ns is the limit of our measurements. This enhanced contribution of the fast time components leading to lowering of the average PL lifetime $\langle\tau\rangle$ is accompanied with a significant deterioration of PL efficiency $\eta_{\mathrm{PL}} \sim I_{\mathrm{int}}/I_{\mathrm{exc}}$ (Fig. 9); thus corroborating our earlier assumption on faster PL decay being due to the contribution of nonradiative processes.

The exact reason(s) of the observed PL efficiency droop are beyond the scope of the current study; this phenomenon is well established in III-nitrides (see [25] and references there) and is widely discussed in the literature. The fact that the samples with strained AlGaN show on average stronger decrease of $\langle\tau\rangle$ while their PL droop is in contrast somewhat weaker in comparison to the samples with relaxed AlGaN (Fig. 9) needs to be commented upon. To understand this behaviour, one can compare the time integrated PL spectra of samples with most strained and least strained AlGaN measured at low cw (Fig. 4) and the highest pulsed excitation energy density (Fig. 10). Having less dislocations, the most strained AlGaN shows some and quite a strong RT PL at this excitation conditions, respectively. This means that the nonradiative channel in the AlGaN is not so strong, and at the highest pulsed excitation at least for short time after the pulse it is partially saturated providing a longer lifetime of own carriers during which holes in barriers are still available for recombination with electrons in QWs. Additionally AlGaN band-edge emission itself can excite extra carriers in QWs further diminishing the overall PL efficiency droop. Obviously in

the case of the samples with relaxed AlGaN both these mechanisms are marginal since nonradiative channels of recombination cannot be saturated manifesting in no cw RT AlGaN band-edge PL and only a weak one at the highest pulsed excitation level.

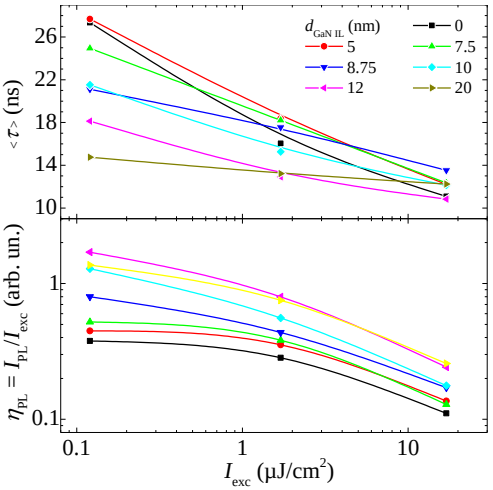

Fig. 9. – Average PL lifetime (see text for definition) and PL efficiency as functions of excitation level.

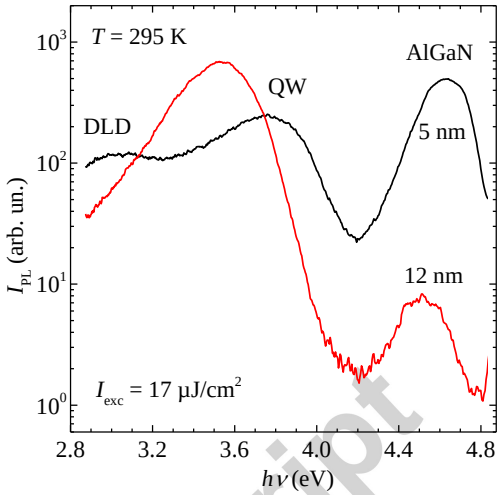

Fig. 10. – RT time integrated PL spectra of two samples at the highest excitation level.

Conclusions

The use of thin GaN interlayers for the relaxation of AlGaN buffer from AlN-template and its effect on the luminescent properties of $In_xAl_{1-x}N/Al_{0.53}Ga_{0.47}N$ MQWs grown subsequently have been investigated. A nominally 10-12 nm thick GaN interlayer was found to be sufficient to fully relax AlGaN with respect to the AlN template while a thicker insertion led to a strong wafer cracking in virtue of tensile strain relief. It is shown that indium incorporation in the InAlN QWs is affected by the strain state of InAlN provided by in-plane lattice parameter of $Al_{0.5}Ga_{0.5}N$ buffer. Lower indium content QWs grown on strained AlGaN buffer being closer to polarisation matching conditions have been found to exhibit longer radiative lifetimes while demonstrating lower PL efficiencies. The observed behaviour can be explained in the framework of idea providing for existing of type I to type II band lineup transition in the InAlN-AlGaN system first proposed in [10] and may serve as a further corroboration of it.

Acknowledgements

This work was enabled by Science Foundation Ireland (SFI) under grant No. SFI/10/IN.1/I2993 and the Irish Higher Education Authority Programme for Research in Third Level Institutions Cycles 4 and 5 via the INSPIRE and TYFFANI projects. SNA acknowledges studentship funding from Iranian Ministry of Science, Research and Technology. PJP acknowledges funding from SFI Engineering Professorship scheme (SFI/07/EN/E001A).

References

[1] H. Hideki, M. Noritoshi, F. Sachie, T. Shiro, K. Norihiko, Recent progress and future prospects of AlGaN-based high-efficiency deep-ultraviolet light-emitting diodes, Japanese Journal of Applied Physics, 53 (2014) 100209.

[2] V. G. Deibuk, A. V. Voznyi, Thermodynamic stability and redistribution of charges in ternary AlGaN, InGaN, and InAlN alloys, Semiconductors, 39 (2005) 623-628.

[3] K. B. Lee, P. J. Parbrook, T. Wang, F. Ranalli, T. Martin, R. S. Balmer, D. J. Wallis, Optical investigation of exciton localization in $Al_xGa_{1-x}N$, Journal of Applied Physics, 101 (2007) 053513.

[4] H. Angerer, D. Brunner, F. Freudenberg, O. Ambacher, M. Stutzmann, R. Höpler, T. Metzger, E. Born, G. Dollinger, A. Bergmaier, S. Karsch, H. -J. Körner, Determination of the Al mole fraction and the band gap bowing of epitaxial AlxGa1−xN films, Applied Physics Letters, 71 (1997) 1504-1506.

[5] L. Sang, M. Liao, M. Sumiya, A comprehensive review of semiconductor ultraviolet photodetectors: from thin film to one-dimensional nanostructures, Sensors, 13 (2013) 10482-10518.

[6] K. P. O'Donnell, R. W. Martin, P. G. Middleton, Origin of Luminescence from InGaN Diodes, Physical Review Letters, 82 (1999) 237-240.

[7] V. Z. Zubialevich, E. V. Lutsenko, V. N. Pavlovskii, A. L. Gurskii, A. V. Danilchyk, G. P. Yablonskii, M. B. Danailov, B. Ressel, A. A. Demidovich, J. F. Woitok, H. Kalisch, Y. Dikme, R. H. Jansen, M. Lünenbürger, B. Schineller, M. Heuken, Mechanisms for spontaneous and stimulated recombination in multiple quantum wells of InGaN/GaN heterostructures on silicon substrates, Journal of Applied Spectroscopy, 75 (2008) 96-103.

[8] S. Keller, S. P. DenBaars, Metalorganic chemical vapor deposition of group III nitrides—a discussion of critical issues, Journal of Crystal Growth, 248 (2003) 479-486.

[9] V. Z. Zubialevich, T. C. Sadler, D. V. Dinh, S. N. Alam, H. N. Li, P. Pampili, P. J. Parbrook, Enhanced UV luminescence from InAlN quantum well structures using two temperature growth, J. Luminesc. 155 (2014) 108–111.

[10] V. Z. Zubialevich, S. N. Alam, H. N. Li and P. J. Parbrook, Composition dependence of photoluminescence properties of $In_xAl_{1-x}N$/AlGaN quantum wells, J. Physics. D, 49 (2016) 385105.

[11] A. Yamamoto, K. Sugita, A. G. Bhuiyan, A. Hashimoto, N. Narita, Metal-organic vapor-phase epitaxial growth of InGaN and InAlN for multi-junction tandem solar cells, Materials for Renewable and Sustainable Energy, 2 (2013) 1-9.

[12] T. C. Sadler, M. J. Kappers, R. A. Oliver, The effects of varying metal precursor fluxes on the growth of InAlN by metal organic vapour phase epitaxy, Journal of Crystal Growth, 314 (2011) 13-20.

[13] T.-T. Kang, M. Yamamoto, M. Tanaka, A. Hashimoto, A. Yamamoto, Effect of gas flow on the growth of In-rich AlInN films by metal-organic chemical vapor deposition, Journal of Applied Physics, 106 (2009) 053525.

[14] T. Y. Wang, J. H. Liang, D. S. Wuu, Defect formation mechanism and quality improvement of InAlN epilayers grown by metal-organic chemical vapor deposition, Cryst. Eng. Comm., 17 (2015) 8505-8511.

[15] H. N. Li, T. C. Sadler, P. J. Parbrook, AlN heteroepitaxy on sapphire by metalorganic vapour phase epitaxy using low temperature nucleation layers, Journal of Crystal Growth, 383 (2013) 72-78.

[16] T. Wang, K. B. Lee, J. Bai, P. J. Parbrook, R. J. Airey, Q. Wang, G. Hill, F. Ranalli, A. G. Cullis, Greatly improved performance of 340 nm light emitting diodes using a very thin GaN interlayer on a high temperature AlN buffer layer, Applied Physics Letters, 89 (2006) 081126.

[17] J. Bai, T. Wang, K. B. Lee, P. J. Parbrook, Q. Wang, A. G. Cullis, Generation of misfit dislocations in highly mismatched GaN/AlN layers, Surface Science, 602 (2008) 2643-2646.

[18] R. A. Coppeta, H. Ceric, D. Holec, T. Grasser, 2013 IEEE International Integrated Reliability Workshop Final Report, 2013, pp. 133-136.

[19] K. Lorenz, N. Franco, E. Alves, S. Pereira, I. M. Watson, R. W. Martin, K. P. O'Donnell, Relaxation of compressively strained AlInN on GaN, Journal of Crystal Growth, 310 (2008) 4058-4064.

[20] W. Jiao, W. Kong, J. Li, K. Collar, T.-H. Kim, A.S. Brown, The relationship between depth-resolved composition and strain relaxation in InAlN and InGaN films grown by molecular beam epitaxy, Applied Physics Letters, 103 (2013) 162102.
[21] S. Pereira, M. R. Correia, E. Pereira, K. P. O'Donnell, C. Trager-Cowan, F. Sweeney, E. Alves, Compositional pulling effects in $In_xGa_{1-x}N/GaN$ layers: A combined depth-resolved cathodoluminescence and Rutherford backscattering/channeling study, Physical Review B, 64 (2001) 205311.
[22] Y. Zhao, J.-C. Zhang, J.-S. Xue, X.-W. Zhou, S.-R. Xu, Y. Hao, Influence of compressive strain on the incorporation of indium in InGaN and InAlN ternary alloys, Chinese Physics B, 24 (2015) 017302.
[23] K. Ohkawa, T. Watanabe, M. Sakamoto, A. Hirako, M. Deura, 740-nm emission from InGaN-based LEDs on *c*-plane sapphire substrates by MOVPE, Journal of Crystal Growth, 343 (2012) 13–16.
[24] W. Paszkowicz, R. Černý, S. Krukowski, Rietveld refinement for indium nitride in the 105–295 K range, Powder Diffraction, 18 (2003) 114-121.
[25] T. Kim, T.-Y. Seong, O. Kwon, Investigating the origin of efficiency droop by profiling the voltage across the multi-quantum well of an operating light-emitting diode, Applied Physics Letters, 108 (2016) 231101.